catalysts

MDPI

Article

High Yield to 1-Propanol from Crude Glycerol Using Two Reaction Steps with Ni Catalysts

Martín N. Gatti, Julieta L. Cerioni, Francisco Pompeo, Gerardo F. Santori and Nora N. Nichio *

Centro de Investigación y Desarrollo en Ciencias Aplicadas (CINDECA) y Facultad de Ingeniería, Universidad Nacional de La Plata-Consejo Nacional de Investigaciones Científicas y Técnicas (UNLP-CONICET), 47 No. 257, La Plata 1900, Argentina; martin.gatti@ing.unlp.edu.ar (M.N.G.); julieta.cerioni@quimica.unlp.edu.ar (J.L.C.); fpompeo@quimica.unlp.edu.ar (F.P.); santori@quimica.unlp.edu.ar (G.F.S.)

* Correspondence: nnichio@quimica.unlp.edu.ar; Tel.: +54-221-422-1878

Received: 26 April 2020; Accepted: 22 May 2020; Published: 2 June 2020

Abstract: The objective of the present work is to achieve high yield to 1-propanol (1-POH) by crude glycerol hydrogenolysis in liquid phase and find an alternative to the use of noble metals by employing Ni catalysts. Two Ni catalysts with different supports, alumina (γ-Al_2O_3), and a phosphorous-impregnated carbon composite (CS-P) were studied and characterized in order to determine their acid properties and metallic phases. With the Ni/γ-Al_2O_3 catalyst, which presented small particles of metallic Ni interacting with the acid sites of the support, it was possible to obtain a complete conversion of crude glycerol with high selectivity towards 1,2-propylene glycol (1,2 PG) (87%) at 220 °C whereas with the Ni/CS-P catalyst, the presence of AlPOx species and the Ni_2P metallic phase supplied acidity to the catalyst, which promoted the C-O bond cleavage reaction of the secondary carbon of 1,2 PG to obtain 1-POH with very high selectivity (71%) at 260 °C. It was found that the employment of two consecutive reaction stages (first with Ni/ γ-Al_2O_3 at 220 °C and then with Ni/CS-P at 260 °C) allows reaching levels of selectivity and a yield to 1-POH (79%) comparable to noble metal-based catalysts.

Keywords: glycerol; hydrogenolysis; 1-propanol; Ni catalyst

1. Introduction

Glycerol is a by-product of biodiesel synthesis and is currently considered an important biomass resource because it can be used as a raw material to synthesize other chemical compounds that, in the past, were obtained by petrochemical methods [1–4]. Particularly, glycerol hydrogenolysis leads to the formation of glycols such as 1,2-propylene glycol (1,2-PG) [5–7] and 1,3-propylene glycol (1,3-PG) [8–10], and propanols 1-propanol (1-POH) and 2-propanol (2-POH) [11–13].

With respect to 1,2-PG, it has been widely used as a raw material in cosmetic, pharmaceutical, food, and chemical industries [14]. No less important is 1-POH, a chemical utilized as an additive in the manufacture of printing inks, antifreezes, brake fluids, and cosmetic lotions that can also be employed as a solvent in the manufacture of rubber, lacquer and essential oils [15].

As previously reported by several authors, 1,2-PG is obtained by a first dehydration stage of C-O bond cleavage reaction from glycerol molecule and a subsequent hydrogenation stage, while 1-POH can be obtained through the subsequent hydrogenolysis of 1,2-PG [16–18]. However, in the literature, there are more scientific contributions focused on glycerol hydrogenolysis to produce 1,2-PG than to produce 1-POH [19,20], though the latter is also a high value-added product [21].

To obtain glycols or 1-POH, a bifunctional catalyst is required. In this reaction, the surface acid-base properties of the support play an important role. On the other hand, the choice of the metallic phase is also relevant. It has been reported that metallic phases based on noble metals such as Ru [22,23],

Pt [24,25], and Pd [26,27] are very active for the hydrogenation of glycerol reaction, although they are expensive and in some cases favor undesirable C-C bond cleavage reactions.

Bhanuchander et al. [12] tested supported Pt catalysts on AlP, TiP, ZrP, and NbP. Among all the catalysts employed, Pt/TiP was found to be the most active one in vapor phase hydrogenolysis at 220°C and 0.1 MPa of H_2, obtaining total glycerol conversion and high selectivity towards 1-POH (~87%) using 10 wt.% glycerol solutions and 1.02 h^{-1} of space velocity (WHSV). These authors attributed the results obtained to the acid strength present in the sites of the TiP support and to the high dispersion of the Pt atoms (particles of average diameter 4 nm). These same conclusions were reported by Priya et al. [11] with Pt catalysts supported over ZrO_2 modified with phosphotungstic acid. These catalysts exhibited high selectivity towards propanols (~98% selectivity towards 1-POH and 2-POH) with total conversion of glycerol at 230 °C, 0.1 MPa of H_2, using dilute glycerol solutions (between 5 and 10 wt.%) and 1.02 h^{-1} of space velocity (WHSV).

Zhu et al. [15], employing Pt catalysts supported over ZrO_2 modified with HSiW, found that propanols can be obtained at 200 °C and 5 MPa of H_2, with high selectivity (~80%) and total conversion of glycerol using 10 wt.% aqueous glycerol solutions and 0.045 h^{-1} of space velocity in a liquid phase continuous flow reactor. These authors attributed the performance of the catalyst to a good balance between acid sites and surface-active species for hydrogenation.

Samudrala et al. [28] investigated Pd/MoO_3-Al_2O_3 catalysts for 1-POH and 2-POH production. They found that the synergic interaction between Pd and MoO_3 on the Al_2O_3 support and the acidity of the catalyst were solely responsible for the high catalytic activity. High glycerol conversion (~88%) with high selectivity to propanols (~91%) was achieved at 210 °C, 0.1 MPa of H_2, and 3 h of reaction using 10 wt.% glycerol.

Ryneveld et al. [19] studied Pd/C and Ru/C catalysts. Pd/C can reach 38% of glycerol conversion with 52% selectivity towards 1-POH, at 250 °C and 8 MPa of H_2 and 24 h of reaction. Ru/C, under the same operative conditions, can reach a ~99% of glycerol conversion with low selectivity towards 1-POH (~18%), due to C-C cleavage bond reactions.

Catalysts based on Ni or Cu have become an interesting alternative due to their capacity for C-O bond cleavage and their lower cost [16]. Ryneveld et al. [20] analyzed Ni supported catalysts over SiO_2 and Al_2O_3. They found that Ni/Al_2O_3 showed the best performance with ~100% conversion of glycerol and ~43% selectivity towards 1-POH at 320 °C, 6 MPa of H_2, and 3 h^{-1} of space velocity (LHSV). The authors assigned this performance to the higher concentration of strong acid sites on the Ni/Al_2O_3 compared to Ni/SiO_2.

In order to increase selectivity to lower alcohols, such as methanol (MeOH), ethanol (EtOH) and 1-POH, Shozi et al. modified Ni/SiO_2 and Ni/Al_2O_3 with 1 wt.% of Re. Among the catalysts tested, Ni-Re/Al_2O_3 favored the formation of 1-POH, reaching 30% yield at 325 °C, 6 MPa of H_2, and 24 h of reaction using 60 wt.% glycerol in a continuous-flow fixed-bed reactor [29]. In another contribution, these authors [30] studied Mo and W catalysts supported on SiO_2 and γ-Al_2O_3. Their work showed the best results using a Mo/SiO_2 catalyst, reaching 42% glycerol conversion with ~40% selectivity towards 1-POH, at 325 °C, 6 MPa of H_2, 60 wt.% glycerol and 10 h^{-1} of space velocity (LHSV).

From the above, it is clear that 1-POH can be obtained through glycerol hydrogenolysis though the yields achieved are relatively lower than those of 1,2-PG. In order to increment the yield towards 1-POH, Lin et al. reported sequential two-layer catalysts in a continuous-flow fixed-bed reactor. An acidic H-β catalyst layer was packed before a Ni/Al_2O_3 catalyst layer in the reactor. These sequential two-layer catalysts provided good 1-POH selectivity (~69%) with complete glycerol conversion at 220 °C, 2 MPa of H_2, and 6.05 h^{-1} of space velocity (WHSV) [31]

A less explored aspect is the effect that the use of crude glycerol from the biodiesel industry might have. Most scientific work has employed analytical glycerol solutions within a wide range of concentrations (10–80 wt.%). However, crude glycerol from the biodiesel industry is always found at high concentrations (70–80 wt.%) and has impurities of a different nature [32–34]. Among those impurities, remnants of methanol and NaOH can come from the biodiesel synthesis [32] as well as

NaCl [33] or Na_2SO_4 [34] due to the neutralization of NaOH with inorganic acids, such as HCl or H_2SO_4 respectively. Matter organic non-glycerol (MONG) such as mono, di- and triglycerides may also be present in crude glycerol [33]. In the case of NaOH, it was reported that the concentration of NaOH can lead to lactic acid formation, which is a degradation product [35]. With respect to the NaCl salt, the presence of Cl- can lead to a catalyst deactivation due to the incorporation of Cl- over the metallic particles [33]. As regards the MONG content, reports indicate that glycerides (mono, di, or triglycerides) make the catalyst surface dirty, block active sites, and even act as coke precursors [33]. In this way, the use of crude glycerol would be an important variable to study a catalytic material for the glycerol hydrogenolysis reaction.

The objectives of the present work are to achieve high yield to 1-POH by crude glycerol hydrogenolysis in liquid phase and to find an alternative to the use of noble metals by employing Ni catalysts. Two Ni catalysts with different supports, alumina, and a carbon composite were studied and characterized in order to determine their acid properties and metallic phases. In this sense, the acidic properties of alumina promote the dehydration of glycerol to acetol ($AcCH_2OH$), which is the main intermediate in the hydrogenolysis reaction. Furthermore, if there is any transformation from alumina to boehmite, due to the hydrothermal conditions of this reaction, this gives it more acidity without negatively affecting the reaction. Carbon-based supports have been widely reported in liquid phase reactions at low temperatures, with advantages associated with their hydrophobicity, stability, textural properties, as well as easy recovery of the metal phase. They can also be acidified by different techniques such as functionalization with inorganic acids [36]. In fact, in previous studies, we found that a carbon composite treated with HF generates the presence of phenolic and lactonic groups on its surface, favoring the formation of 1-POH [37].

For each catalyst, the operative reaction conditions were optimized to reach total conversion and the higher selectivity to the main product.

Taking into consideration that 1,2 PG is the intermediate compound to produce 1-POH, the possibility of employing both catalysts was analyzed, using two consecutive reaction stages.

2. Results and Discussion

2.1. Characterization of Supports and Catalysts

Figure 1 shows the X-ray diffractograms of the supports: γ-Al_2O_3 and phosphorous-impregnated carbon composite (CS-P). For the γ-Al_2O_3 support, the main peaks are observed at 2θ = 18.9°, 32.5°, 36.9°, 39.1°, 45.3°, 59.6° and 66.7° characteristic of this low crystallinity aluminum oxide (●) (JCPDS 04-0858).

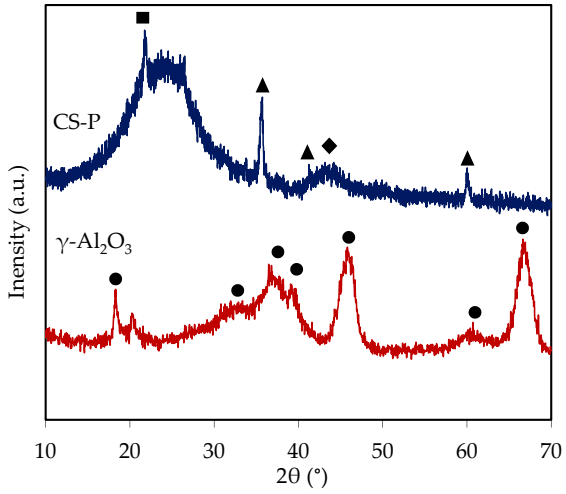

Figure 1. XRD of supports; symbols are referred to aluminum oxide (●), tridymite (■), silicon carbide (▲) and graphitic carbon (♦).

In the CS-P composite, a peak at 2θ = 43.7° can be observed that is assigned to the hexagonal phase of graphite carbon (♦) (JCPDS 25-284). The presence of graphitic carbon is due to the pyrolysis in reducing atmosphere of the phenol-formaldehyde liquid resin employed for the synthesis of the CS support (more details in Supplementary Materials). An amorphous plateau between 2θ = 15° and 30° that is characteristic of amorphous silica is also observed, and a peak at 2θ = 21.8° that is assigned to the tridymite phase of silica (■) (JCPDS 18-1170). The presence of silica is due to the use of TEOS in the synthesis of the CS support. Besides, the peaks at 2θ = 35.7°, 41.4° and 60.0° can be assigned to silicon carbide (▲) (JCPDS 22-1316). The formation of silicon carbide is explained due to a reaction between carbon and silica during the calcination process at 1580 °C.

Since it was not possible to observe phosphorus phases on the CS-P support, this composite was analyzed by NMR spectroscopy. Figure 2 shows the ^{31}P-NMR spectra for the CS-P support that presents a band at −27 ppm, which is associated with the presence of several orthophosphate species, generally denoted as AlPOx [38,39].

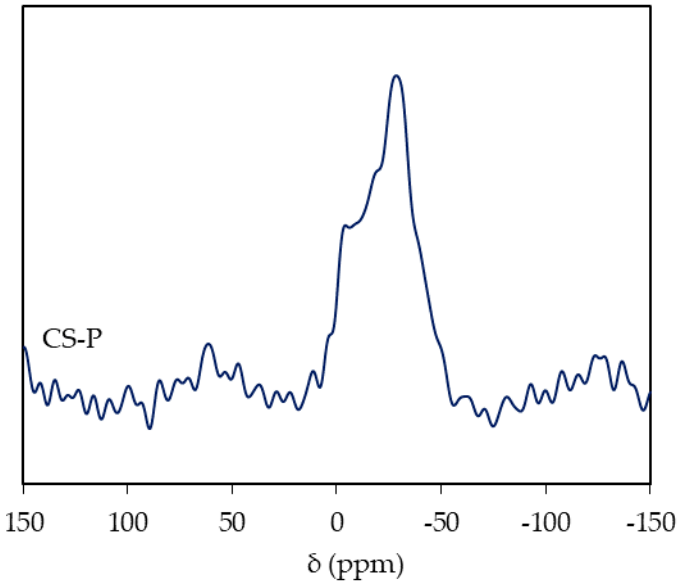

Figure 2. ^{31}P-NMR spectra of the CS-P support.

Table 1 shows the textural characterization of the supports by the adsorption-desorption of N_2 and the surface acid properties determined by the decomposition reaction of isopropanol (IPA) and potentiometric titration.

Table 1. Textural and acid-base properties of supports.

Support	BET		Potentiometric Titration		IPA Decomposition Reaction (X_{IPA} = 15 %)			
	S_{BET} [a]	V_p [b]	Ei [c]	NS [d]	T [e]	$S_{propylene}$ [f]	$S_{acetone}$ [g]	S_{DIPE} [h]
γ-Al_2O_3	185	0.50	60	0.35	200	73	0	27
CS-P	235	0.70	340	0.59	170	100	0	0

[a] Specific surface area (m^2 g^{-1}) [b] Total pore volume (cm^3 g^{-1}) [c] Initial potential (mV) [d] Total number of acid sites (mmol n-butylamine g^{-1}) [e] Temperature (°C) [f] Selectivity to propylene (%) [g] Selectivity to acetone (%), [h] Selectivity to di-isopropyl ether (%).

The adsorption-desorption isotherms of N_2 for γ-Al_2O_3 and CS-P were of type IV, characteristic of mesoporous materials with hysteresis loops H1 and H3, respectively. Isotherms and pore size distributions are shown in Supplementary Figures S1 and S2.

Although the supports have a similar porosity around 200 m^2 g^{-1}, they present greater differences in their acidic surface properties. Although carbonaceous supports generally have specific surface area

(S_{BET}) values greater than 600 m^2 g^{-1}, the lower S_{BET} in the support impregnated with $Al(H_2PO_4)_3$ (CS-P) can be ascribed to a partial blocking of pores. Araujo et al. also reported that the impregnation with phosphoric acid noticeably reduced the mesoporous volume of the support [40].

The potentiometric titration technique with n-butylamine allowed determining the strength of the acid sites and the total number of acid sites present in a given solid. While the initial potential of the titration curve (Ei) indicates the maximum strength of the acid sites, the consumption of n-butylamine is related to the total number of acid sites (NS). The γ-Al_2O_3 and CS-P supports present Ei values of 60 and 340 mV respectively. This indicates that the superficial acid sites are strong and very strong for γ-Al_2O_3 and CS-P respectively [37]. In Table 1, it can be seen that the CS-P support has a higher total number of acid sites (NS) than the γ-Al_2O_3 support.

The decomposition reaction of isopropanol (IPA) is known as an indirect method that allows characterizing the acid strength and type of sites of the surface of a solid. These are classified according to their ability to dehydrate and form propylene, di-isopropyl ether (DIPE) and/or acetone, or to dehydrogenize and form acetone and hydrogen.

As observed in Table 1, to achieve an IPA conversion level of 15%, the CS-P support requires a temperature of 170 °C, while γ-Al_2O_3 requires 200 °C. The lower the temperature to reach a certain level of conversion, the greater the number of surface active sites [41].

On the other hand, the selectivity analysis towards the different reaction products allows determining the nature of the surface active sites. As observed in Table 1, the γ-Al_2O_3 support has a selectivity of 73% towards propylene and 27% towards DIPE, which would indicate that this material has strong Lewis acid sites. The CS-P support exhibits 100% selectivity towards propylene, indicating the presence of strong Lewis and/or Brønsted acid sites [41]. Because NMR spectroscopy shows AlPOx species, the Lewis acidity could be assigned to cations Al^{+3} and the Brønsted acidity to the P-OH groups, as reported by Moffat et al. [42].

As regards the Ni catalysts, Table 2 shows the results of the textural and physicochemical characterization.

Table 2. Textural and physical-chemical properties of catalysts.

Catalyst	AAS	BET		Potentiometric Titration		XRD	TEM	TPR		
	Ni [a]	S_{BET} [b]	V_p [c]	Ei [d]	NS [e]	d_{XRD} [f]	d_{va} [g]	T_1 [h]	T_2 [h]	T_3 [h]
Ni/γ-Al_2O_3	4.8	174	0.50	36	0.30	n.d.	4	322	532	625
Ni/CS-P	5.2	395	0.80	118	0.50	11	12	-	-	-

[a] Ni content (wt.%) [b] Specific surface area (m^2 g^{-1}) [c] Total pore volume (cm^3 g^{-1}) [d] Initial potential (mV) [e] Total number of acid sites (mmol n-butylamine g^{-1}) [f] Crystallite size (nm) [g] Average particle diameter (nm) [h] Temperature of 1st, 2nd and 3rd peak in TPR analysis (°C).

By the AAS technique, it was determined that in both catalysts, the Ni content was very close to the nominal value (5 wt.%).

The results of the adsorption-desorption of N_2 show a drop in the value of S_{BET} for the reduced Ni/γ-Al_2O_3 catalyst, which is due to the blocking of the pores due to the presence of Ni. Conversely, for the Ni/CS-P catalyst, there is an increase in $S_{BET,}$ which could be assigned to the loss of some $AlPO_x$ species of the support, during the thermal treatment in H_2 flow, that were blocking the support pores. It has been reported in the literature that the thermal treatment of phosphoric acid species in carbon is employed to increase the specific area [43]. Isotherms and pore size distributions of the catalysts are shown in Supplementary Figures S1 and S2.

The results of the potentiometric titration (Table 2) indicate the preservation in the catalysts of the strong acid sites of the supports. Thus, the Ni/CS-P catalyst has a greater number of acid sites than Ni/γ-Al_2O_3 and a higher acid strength of the sites.

Figure 3 shows the X-ray diffractograms of the reduced catalysts. For the Ni/γ-Al_2O_3 catalyst, a peak at 51.7° is observed which corresponds to the Ni metal phase (▼) (JCPDS 4-850). Due to the low

intensity of this peak, it was not possible to calculate an average crystallite size (using the Scherrer equation) but this would indicate that these particles are widely dispersed.

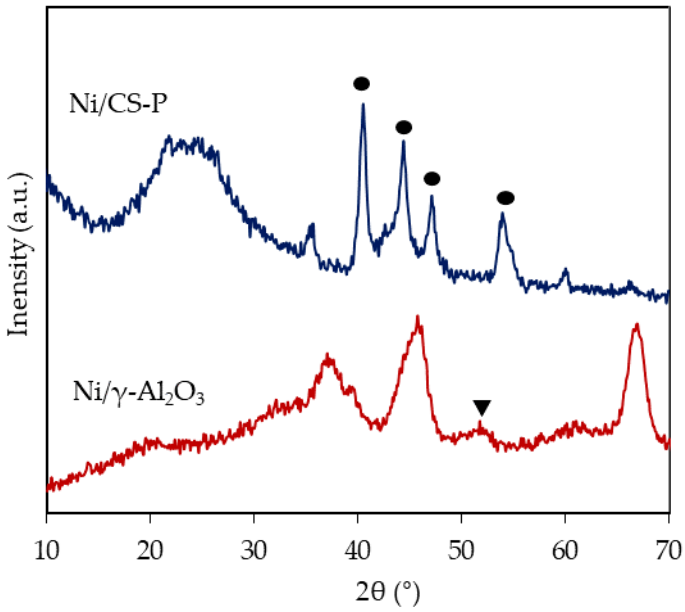

Figure 3. XRD of reduced catalysts; symbols are referred to Ni_2P phase (●) and metallic Ni (▼).

In the X-ray diffractogram of the Ni/CS-P catalyst, the peaks at 2θ° = 40.6°, 44.5°, 47.1° and 54.1° that correspond to the Ni_2P phase (●) can be observed (JCPDS 74-1385). Several publications have reported that in Ni and P catalysts, the Ni/P molar ratio would determine the type of alloy formed. For Ni/P ratios greater than 1.4, the formation of the $Ni_{12}P_5$ and Ni_3P phases has been indicated, while for Ni/P ratios less than 1, the formation of the Ni_2P phase has been reported [44,45]. Since the Ni/CS-P catalyst has a Ni/P molar ratio equal to 0.36, it would be in agreement with the formation of the Ni_2P phase determined by XRD. The average crystallite size of Ni_2P is about 11 nm, obtained by the Scherrer equation, using the peak at 40.6 ° corresponding to plane (111) of Ni_2P.

Since the moles of P with respect to Ni are greater, in the Ni/CS-P catalyst all Ni is alloyed as Ni_2P and P unalloyed as AlPOx species, even though it was not possible to detect these latter species by XRD. While AlPOx species were detected in the support by NMR, it was not possible to apply this technique in the catalyst due to the magnetic properties of Ni.

Figure 4 shows the TEM images and the particle size distribution for the reduced catalysts. For the Ni/γ-Al_2O_3 catalyst, the histogram shows a narrow distribution with particle sizes between 3 and 5 nm, while the Ni/CS-P catalyst has a wider distribution, with particles from 3 to 21 nm. Table 2 shows the average particle diameter values, where Ni/γ-Al_2O_3 catalyst has an average diameter of 4 nm. In contrast, the Ni/CS-P catalyst has an average diameter of 12 nm, which is a value very similar to the crystallite size determined by XRD.

The TPR results are summarized in Table 2. As observed, the Ni/γ-Al_2O_3 catalyst has three characteristic peaks. The first of them at 322 °C indicates the presence of low interaction NiO with the support. The second peak, at 532 °C, would indicate the reduction of Ni^{+2} ions incorporated in the octahedral vacancies of γ-Al_2O_3. Finally, the third peak at 625°C indicates the reduction of Ni^{+2} with high interaction with the support [46,47]. TPR peaks assigned to nickel oxides that are not completely integrated in the spinel structure, but have a certain degree of interaction with the support, were observed at temperatures between 500 and 600 °C [48].

As we have indicated, Ni/CS-P was directly activated in H_2 flow (50 cm^3 min^{-1}) at 400 °C during 90 min, so the TPR analysis would allow to verifying the reduction of the metal phase. Indeed, no peak was observed, indicating that the activation method was effective to reduce all the Ni precursor.

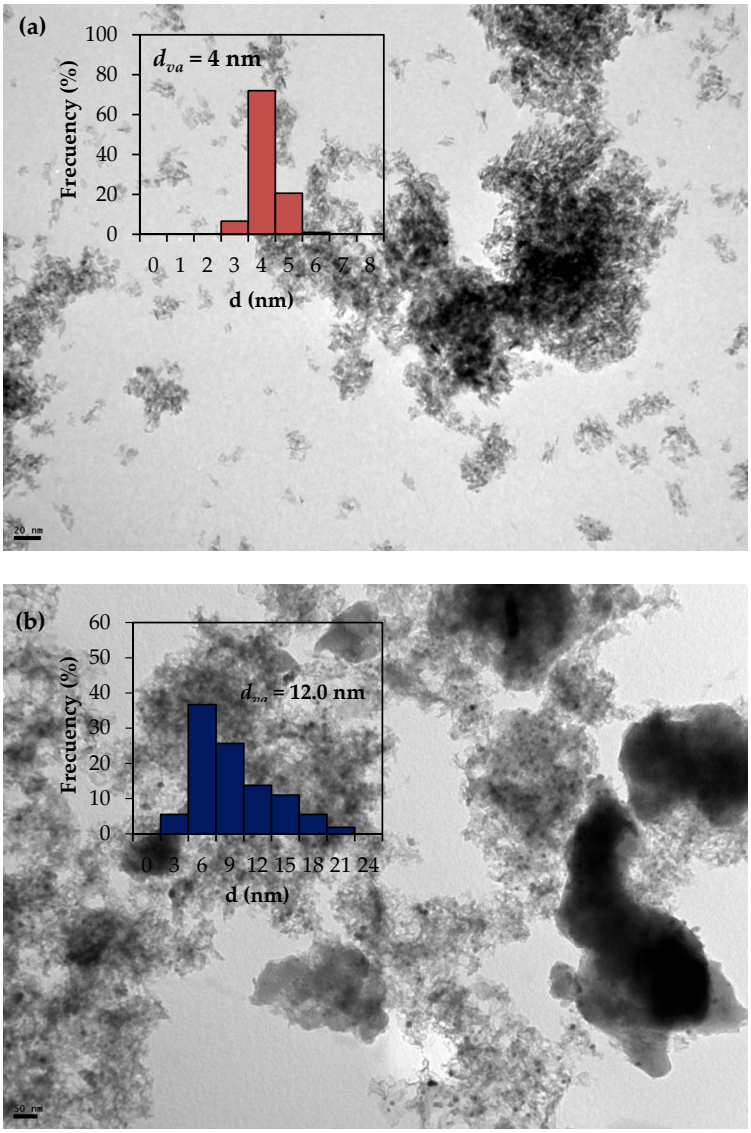

Figure 4. TEM micrographs and particle size distribution of catalysts: (**a**) Ni/γ-Al_2O_3 (**b**) Ni/CS-P.

2.2. Catalytic Activity

The catalytic activity tests were carried out using both technical grade glycerol (99 % Cicarelli) and crude glycerol (Oleomud). The composition of this crude glycerol (~79 wt.%) is shown in Table 3. This raw material contains MeOH and MONG from the biodiesel manufacturing process. The MONG content includes MeOH, mono-, di-, triglycerides, etc. The ash content is mainly due to the presence of Na^+ salts produced during the neutralization of the NaOH catalyst with acid.

Table 3. Characterization of crude glycerol.

Parameter	Value
pH	6.0
Density	1.257
Glycerol content (wt.%)	79.3
Methanol content (wt.%)	2.0
MONG (wt.%)	6.7
Water content (wt.%)	11.0
Ash content (wt.%)	3.0

Catalytic activity results in the glycerol hydrogenolysis reaction are shown in Table 4.

Table 4. Glycerol hydrogenolysis.

Test	Gly (wt.%)	T(°C)	t(h)	X (%)	Selectivity (%)								CB [c] (%)
					Gases	MeOH	EtOH	AcO	1-POH	$AcCH_2OH$	EG	1,2-PG	
$Ni/\gamma\text{-}Al_2O_3$ catalyst													
1	10	200	2	10.0	0.0	1.2	3.6	0.0	0.4	0.5	19.2	75.1	93
2	10	220	2	22.0	1.8	0.9	6.8	0.0	0.0	0.3	12.6	77.6	95
3	10	260	2	44.7	20.1	10.7	20.4	5.7	6.5	0.2	26.8	9.6	96
4	80	220	2	40.0	1.3	0.4	5.2	0.0	0.3	2.1	4.0	86.7	96
5	80	220	5	100.0	3.0	0.7	4.0	1.0	1.2	0.2	6.8	83.0	97
6	80 [a]	220	5	100.0	3.2	0.5	2.4	0.1	0.1	0.0	6.7	87.0	97
Ni/CS-P catalyst													
7	10	220	2	4.9	0.5	0.1	1.0	0.3	19.3	0.8	0.0	78.0	96
8	30	260	2	37.9	1.5	0.3	4.4	19.8	64.5	5.3	0.0	4.2	96
9	80	260	2	45.1	1.3	0.4	4.0	22.0	67.0	4.0	0.0	1.3	96
10	80 [a]	260	5	100.0	1.1	0.1	3.7	23.0	71.0	1.0	0.0	0.0	97
11	80 [b]	260	2	100.0	1.5	0.0	1.1	2.3	91.0	4.4	0.0	0.0	97
$Ni/\gamma\text{-}Al_2O_3$ catalyst + Ni/CS-P catalyst Two consecutive reaction tests: 5 h 220 °C with $Ni/\gamma\text{-}Al_2O_3$ catalyst followed by 2 h at 260 °C with Ni/CS-P catalyst													
12	80 [a]	220–260	7	100.0	6.0	1.4	4.5	2.4	79.3	0.0	6.5	0.0	97

Reaction conditions: m_c/m_{gly} = 0.16 (mass ratio), pH_2 = 6.5 MPa. [a] Crude glycerol Oleomud [b] with reaction mixture 80 wt.% 1,2-PG [c] carbon balance.

The reaction products in liquid phase that were identified and quantified were the following: from C1: methanol (MeOH), from C2: ethanol (EtOH), ethylene glycol (EG), from C3: acetone (AcO), 1-propanol (1-POH), acetol ($AcCH_2OH$), and 1,2-propylene glycol (1,2-PG). The main gaseous products identified were CO_2 and CH_4.

The results of Tests 1–6 were obtained by employing the $Ni/\gamma\text{-}Al_2O_3$ catalyst. It can be seen that with this catalyst it was not possible to obtain 1-POH as the main product. However, the results in Table 4 indicate that, when the temperature is below 260 °C, the main product of glycerol hydrogenolysis is 1,2-PG (Tests 1,2, and 4–6).

At 260 °C (Test 3), it can be observed that there is a strong increase in the products of C1 and C2 (Gases (CH_4 and CO_2), MeOH, EtOH and EG), which shows the greater contribution of the C-C bond cleavage reactions. The $Ni/\gamma\text{-}Al_2O_3$ catalyst has widely dispersed Ni^0 particles with average sizes of 4 nm, and this would promote C-C bond cleavage reactions.

The selectivity towards 1,2-PG reaches its maximum value (77.6%) at the temperature of 220 °C (Test 2). Similarly, Marinoiu et al. employed a $Ni/SiO_2\text{-}Al_2O_3$ catalyst in the range 170–250 °C at 1.5 MPa of H_2 and found that the yield to 1,2-PG reaches a maximum at 200 °C, due to a good balance between conversion and selectivity [49]. In this sense, Menchavez et al. employed a Ni/CeO_2-MgO catalyst and reported that 1,2-PG selectivity was optimal in the range 200–215 °C at 6 MPa of H_2, due to a balance between dehydration and hydrogenation reactions [50].

Furthermore, Long et al. used a Ni catalyst supported on a sepiolite modified with WO_3 and reported that at temperatures higher than 200 °C the selectivity to EG increases due to C-C bond cleavage reactions [51].

From Table 4, the results at 220 °C can be compared with different concentrations of glycerol (Tests 2 and 4), where it is observed that the level of conversion and selectivity improves with the lower content of water in the reaction mixture. Dasari et al. reported that with a $Cu\text{-}Cr_2O_4$ catalyst, the glycerol conversion increases from 33% to 69%, if the water content decreases from 80 wt.% to 0 wt.% (at 200 °C, 1.4 MPa of H_2 and 24 h of reaction) [16]. Menchavez et al. employed a Ni/CeO_2-MgO catalyst and reported an increase in glycerol conversion from 43% to 80% when the water content declined from 40 wt.% to 0 wt.% (at 215 °C, 6.9 MPa of H_2 and 24 h of reaction) [50].

In addition, in Table 4 it can be seen that using a glycerol solution (99% Cicarelli) at 80 wt.% and 220 °C (Test 5), it is possible to obtain total glycerol conversion with a 1,2-PG selectivity of 83%, after 5 h of reaction, which implies a yield towards 1,2-PG of 83%. This yield is superior to the ones reported in the literature for Ni-Raney (68.8%) and Ni/NaX (69.6%) catalysts [52,53].

The results of the hydrogenolysis of crude glycerol (79 wt.% Oleomud) employing the Ni/γ-Al_2O_3 catalyst (Test 6) show that the total conversion of glycerol is also achieved with a selectivity towards 1,2-PG of 87%. The quality of this raw material, which contains impurities such as MeOH and Na^+ salts, slightly affects the results and this presence could have a positive effect. Feng et al. [54] determined that the addition of Li, Na, and K bases to the reaction medium improves the conversion of glycerol following the order: $Li^+ > Na^+ > K^+$. With respect to MeOH, its presence in the reaction medium has been reported to be beneficial due to its H_2 donor capacity [55].

The second part of Table 4 (Tests 7–11) shows the results of the glycerol hydrogenolysis reaction using the Ni/CS-P catalyst. Results obtained at 220 °C with a 10 wt.% glycerol aqueous solution (Test 7) show that Ni/CS-P catalyst is much less active than Ni/γ-Al_2O_3 catalyst (5% vs. 22% conversion), which could be due to the greater metallic dispersion of Ni/γ-Al_2O_3. However, in the tests carried out at higher temperatures and higher glycerol concentrations, it is possible to observe that the Ni/CS-P catalyst does not favor C-C cleavage reactions, and the selectivity to C3 products of glycerol hydrogenolysis is very high. The results of Tests 8–10 show that, with this catalyst, it is possible to obtain 1-POH as the main product of glycerol hydrogenolysis and the main byproduct is AcO. The presence of AcO is explained precisely by the high capacity of C-O bond cleavage of this catalyst.

As reported [16–18], 1,2-PG is the intermediate to form 1-POH and both are the main products of glycerol hydrogenolysis. This is corroborated with the results of Test 11 (Table 4) carried out with an 1,2-PG aqueous solution at 80 wt.%, in which a selectivity towards 1-POH greater than 90% is obtained and there is a very small amount of AcO if compared to the glycerol-fed reaction.

The presence of strong acid sites in the Ni/CS-P catalyst would favor the C-O bond cleavage reactions of the secondary carbon, promoting the formation of 1-POH [37]. On the other hand, the results obtained by XRD evidenced the presence of Ni_2P in the Ni/CS-P catalyst. In the literature, it has been reported that the formation of a NiP alloy provokes an increment in the electrophilicity of Ni sites due to the charge transfer from nickel to phosphorous [56,57]. This property facilitates the adsorption of the O atom of the C-O bond, subsequently promoting the C-O bond cleavage reactions. This tendency increases in the sequence $Ni_3P < Ni_{12}P_5 < Ni_2P$, indicating that for Ni_2P the activity to C-O bond cleavage reactions is the highest among the different nickel phosphides [58]. With respect to the low contents of C1 and C2 reaction products, it was also found that Ni_2P has a much lower activity for the C-C bond cleavage than Ni^0 [58,59]. Furthermore, the Ni/CS-P catalyst has particles with an average size of 12 nm, which is also a disadvantage for C-C bond cleavage reactions.

At 260 °C and after 5 h of reaction (Test 10), a yield to 1-POH of 71% can be obtained, comparable with other catalytic systems reported in the literature such as Pt/$Zr_{0.7}Al_{0.3}O_y$ [13], and this is a yield superior to that obtained with Ni/SiO_2 and Ni/Al_2O_3 [20], Pd/MoO_3-Al_2O_3 [28], Pt/HSiW-Al_2O_3 [21], and Pt/PTA-ZrO_2 [11].

To combine the greater catalytic activity of both catalysts, Ni/γ-Al_2O_3 and Ni/CS-P, to obtain 1,2-PG and 1-POH respectively, we proposed the reaction in two consecutive steps. In this way, we sought to increase the 1-POH yield above 71% which was the maximum that could be obtained with the Ni/CS-P catalyst.

In the first reaction step, the crude glycerol hydrogenolysis reaction was carried out in order to maximize the yield to 1,2-PG, using the Ni/γ-Al_2O_3 catalyst (Test 6). The second stage was carried out with the reaction products obtained from the first stage this time using the Ni/CS-P catalyst (Test 12). The gaseous products (such as CH_4, CO_2) produced in the first stage are the only reaction products that are lost because it is necessary to open the reactor to proceed with the replacement of the catalyst.

To calculate the selectivity to gaseous products reported in Test 12, the moles of gaseous products from the first reaction step were considered (Test 6).

As observed (Table 4), after the second reaction stage a 1-POH yield of 79.3% is achieved (Test 12). Considering both reaction steps, the yield at 1-POH was comparable to that of Pd/CoO catalysts (~80%) [26].

3. Materials and Methods

3.1. Synthesis of Supports and Catalysts

Commercial γ-Al_2O_3 (99.99%, Dytech, Corporation Ltd., Sheffield, UK) and a carbonaceous-based composite were used as supports.

The carbonaceous-based composite was synthetized using the gelling property of TEOS (SILBOND 40-AKZO Chemicals (Buenos Aires, Argentina) in ethanol to include a phenol-formaldehyde liquid resin (RL 43003, ATANOR, Santa Fe, Argentina) in its structure. The Supplementary Materials describe the preparation method used. This material was then modified by impregnation with an $Al(H_2PO_4)_3$ aqueous solution Sigma-Aldrich (St. Louis, MI, USA). The concentration of P in the solution was calculated so as to obtain 7 wt.% P in the final solid. Finally, the solid was dried at 120 °C for 12 h and calcined at 400 °C for 30 min (heating rate of 10 °C min^{-1}). Thus, this support was denoted as CS-P.

The Ni/γ-Al_2O_3 catalyst was prepared by incipient wetness impregnation employing $Ni(NO_3)_3{\cdot}6H_2O$ (Sigma-Aldrich), while the Ni/CS-P catalyst was prepared using $Ni(CH_3COO)_2{\cdot}4H_2O$ in order to decompose this nickel precursor at a lower temperature so as to avoid the gassing of the carbonaceous support.

The concentration of Ni in the solution was calculated so as to obtain 5 wt.% Ni in the final solid. The catalysts were dried at 120 °C during 12 h. Ni/γ-Al_2O_3 was calcined in stagnant air at 550 °C for 90 min (heating rate of 10°C min^{-1}) and activated in H_2 flow (50 cm^3 min^{-1}) at 550 °C for 90 min (heating rate of 10°C min^{-1}). Ni/CS-P was directly activated in H_2 flow (50 cm^3 min^{-1}) at 400 °C for 90 min (heating rate of 10°C min^{-1}) so as to prevent support gasification during the calcination process.

3.2. Characterization of Supports and Catalysts

The adsorption-desorption measurements were carried out employing N_2 at –196 °C for the textural characterization. A Micromeritics ASAP 2020 equipment (Micromeritics Instrument Corporation, Norcross, GA, USA) was employed for the specific surface measurements and micro and mesoporous characterization. The samples were pretreated under vacuum in two 1-h stages at 100 °C and 300 °C, respectively.

The X-ray diffractograms were recorded on a Philips 1729 powder diffractometer, using CuKα radiation (λ = 1.5418 Å, intensity = 20 mA, and voltage = 40 kV). Spectra were collected in the range 2θ = 10–70°. The crystallite sizes (d_{XRD}) in the reduced samples were calculated using the Scherrer equation:

$$d_{XRD} = \frac{K \times \lambda}{B \times cos(\theta)} \quad (1)$$

where K was taken as 0.90 and B was the full width of the diffraction line at half maximum intensity.

The solid-state NMR experiments were performed at room temperature in a 7 T Bruker Avance II-300 spectrometer (Billerica, MA, USA) equipped with a 4-mm MAS probe. The operating frequency for ^{31}P was 121.5. $AlPO_4$ was used as an external reference. ^{31}P 1D spectra were recorded using a π/2 pulse (4.8 μs) and a 30 s delay between two pulses. The spinning rate for the samples was 10 kHz.

The potentiometric titrations were performed employing 0.05 g of sample suspended in acetonitrile (Merck KGaA, Darmstadt, Germany) previously stirred for 3 h. The titrations were suspended with solutions of n-butylamine 0.05 M in acetonitrile, employing a Metrohm 794 Basic potentiometric titrator with a double junction electrode.

The acid-base properties of the supports were determined by the isopropanol (IPA) decomposition test reaction and the potentiometric titration technique. The IPA decomposition test reaction was

carried out in a continuous flow reactor at atmospheric pressure between 120 and 350 °C, employing an IPA flow (4.5%) in helium (40 cm^3 min^{-1}).

The Ni content in the samples was determined by atomic absorption spectrometry (Spectrophotometer AA-6650 Shimadzu, Tokyo, Japan) employing an IL Model 457 spectrometer with single channel and single beam.

Temperature-programmed reduction experiments (TPR) were carried out using conventional equipment. Samples were heated from room temperature up to 800 °C with a heating rate of 10 °C min^{-1} in a mixture of H_2/N_2 (1/9 ratio) with a flow of 50 cm^3 min^{-1}. The H_2 uptake was calculated using a thermal conductivity detector (TCD) previously calibrated.

Images were obtained by electronic transmission microscopy with a TEM JEOL 100 C instrument (JEOL Ltd., Tokyo, Japan) operating at 200 kV. The samples were suspended in 2-propanol and sonicated in an ultrasonic bath during 10 min prior to analysis. In order to estimate average diameter volume/area (d_{va}), the particles were considered spherical and the following expression was used for the calculation:

$$d_{va} = \frac{\sum n_i \times d_i^3}{\sum n_i \times d_i^2} \quad (2)$$

where n_i is the number of particles with diameter d_i. The particle size distribution histograms were obtained from micrographs employing the bright field technique.

3.3. Crude Glycerol Characterization

Crude glycerol was supplied by Olemud S.A., a chemical plant situated in Buenos Aires, Argentina. The density, pH, and the contents of glycerol, methanol, water, ashes, and MONG (Matter Organic Non-Glycerol) of the crude glycerol were measured.

The pH of the sample was determined using a 1 g of crude glycerol dissolved in 50 mL of distilled water and was measured with a digital pH-meter (Oakton pH 11 series, Vernon Hills, IL, USA) at room temperature.

Density was determined using a pycnometer at room temperature (ASTM 891-95). Glycerol and methanol content were determined using a Shimadzu GCMS-QP505A gas chromatograph (Shimadzu Corporation, Tokyo, Japan) equipped with a 50-m 19091S-001 HP PONA capillary column and FID detectors. Water content was measured using a Karl-Fisher titrator (SI Analytics TitroLine Alpha 20 Plus, Xylem Analytics, Weilheim, Germany) (ISO 2098-1972). Ash content was determined by burning 1 g of crude glycerol in a muffle at 750 °C for 3 h (ISO 2098-1972). MONG content was calculated as follows (ISO 2464-1973):

$$MONG\ (wt.\%) = 100 - glycerol\ content\ (wt.\%) - ash\ content\ (wt.\%) - water\ content\ (wt.\%) \quad (3)$$

3.4. Catalytic Actitivy

The activity tests were carried out with a BR-100 (Berghof, Eningen, Germany) high-pressure stainless-steel batch reactor of 100 cm^3. The magnetic stirring was fixed at 1000 rpm in order to ensure the kinetic control conditions.

The Ni/γ-Al_2O_3 and Ni/CS-P catalysts were reduced ex situ in H_2 flow and then cooled down to room temperature under hydrogen flow and immediately transferred to the reactor containing the glycerol. Finally, the reactor was closed, purged, and pressurized with H_2 (Air Liquide, 99.99%) up to the desired pressure. Afterwards, heating was started (6 °C min^{-1}) and, when the reactor was at the desired temperature, the stirring began.

After reaction, the reactor was cooled down to ambient temperature. Gas samples were passed through a pipe with silica-gel so as to dry them and injected into a Shimadzu GC-8A gas chromatograph (Shimadzu Corporation, Tokyo, Japan) equipped with a thermal conductivity detector (TCD) and a Hayesep D 100–120 column operating isothermally at 40 °C. For the identification and quantification

of gas samples, standards of CO, CO_2, and CH_4 were used. Response factors for gas products were obtained using a calibration curve of the standards.

Once the gas samples were analyzed, the reactor was opened under hood, the catalyst was filtered and the liquid obtained was centrifuged and diluted in water (1:40). The liquid samples were injected into a Shimadzu GCMS-QP505A gas chromatograph equipped (Shimadzu Corporation, Tokyo, Japan) with a 50-m 19091S-001 HP PONA capillary column and FID detector. The identification of liquid products was performed by injecting aqueous solutions of the standards at 4 wt.%. The following heating program was used: from 50 °C to 150 °C with a ramp of 10 °C min^{-1}, then from 150 °C to 220 °C with a ramp of 40 °C min^{-1} and then isothermally at 220 °C up to the end of the analysis. The quantification was performed employing the integration of the areas of each compound multiplied by a response factor calculated according to the effective carbon number (ECAN) of each compound, as indicated by Scanlon and Willis [60].

The glycerol conversion (X) was determined as follows:

$$\text{Conversion } (\%) = \frac{\text{moles of consumed glycerol}}{\text{moles of initial glycerol}} \times 100\% \quad (4)$$

The selectivity to liquid products was defined as:

$$\text{Selectivity to specific product } (\%) = \frac{\text{moles of carbon in specific product}}{3 \times \text{ moles of consumed glycerol}} \times 100\% \quad (5)$$

The yield was defined as:

$$\text{Yield to specific product } (\%) = \frac{\text{Selectivity to specific product} \times \text{Conversion}}{100} \quad (6)$$

The carbon balance for all the tests was in the range between 93 and 97 %.

4. Conclusions

The aim of this study was to obtain 1-POH by the hydrogenolysis of crude glycerol using two consecutive reaction stages with Ni catalysts, so as to selectively obtain 1,2 PG in the first stage, which is the intermediate compound necessary to obtain 1-POH in the second stage.

With the Ni/γ-Al_2O_3 catalyst, which presented small particles of metallic Ni interacting with the acid sites of the support, it was possible to obtain a complete conversion of crude glycerol with high selectivity to 1,2 PG (87%) at 220 °C, whereas with the Ni/CS-P catalyst, the presence of AlPOx species and the Ni_2P metallic phase supplied acidity to the catalyst, which promoted the C-O bond cleavage reaction of the secondary carbon of 1,2-PG to obtain 1-POH with very high selectivity (71%) at 260 °C.

It was found that the employment of two consecutive reaction stages (first with Ni/ γ-Al_2O_3 at 220 °C and then with Ni/CS-P at 260 °C) allows reaching levels of selectivity and a yield to 1-POH (79%) comparable to noble metal-based catalysts.

Supplementary Materials: The following are available online at http://www.mdpi.com/2073-4344/10/6/615/s1, Synthesis of CS support, Figure S1: N_2 adsorption-desorption isotherms for (a) CS-P and Ni/CS-P (b) γ-Al_2O_3 and Ni/γ-Al_2O_3. Figure S2: Pore size distribution according to the BJH model for (a) CS-P and Ni/CS-P calculated from the adsorption branch, assuming slit-shape pore geometry (b) γ-Al_2O_3 and Ni/γ-Al_2O_3 calculated from the desorption branch, assuming cylinder-shape pore geometry.

Author Contributions: M.N.G. and J.L.C. carried out all the experimental work which was conceived and designed with G.F.S. and F.P.; N.N.N. wrote the paper. All authors have read and approved the final manuscript.

Funding: This research was conducted with financial support from: "Consejo Nacional de Investigaciones Científicas y Técnicas" (CONICET-PIP 0065) and "Universidad Nacional de La Plata" (UNLP-I-248).

Conflicts of Interest: The authors declare no conflict of interest.

References

1. Chheda, J.N.; Hubert, G.W.; Dumesic, J.A. Liquid-phase catalytic processing of biomass-derived oxygenated hydrocarbons to fuels and chemicals. *Angew. Chem. Int. Edit.* **2007**, *46*, 7164–7183. [CrossRef] [PubMed]
2. Zhou, C.H.; Beltrami, J.N.; Fan, Y.X.; Lu, G.Q. Chemoselective catalytic conversion of glycerol as a biorenewable source to valuable commodity chemicals. *Chem. Soc. Rev.* **2008**, *37*, 527–549. [CrossRef] [PubMed]
3. Hamzah, N.; Nordin, N.M.; Nadzri, A.H.A.; Nik, Y.A.; Kassim, M.B.; Yarmo, M.A. Enhanced activity of Ru/TiO_2 catalyst using bisupport, bentonite-TiO_2 for hydrogenolysis of glycerol in aqueous media. *Appl. Catal. A Gen.* **2012**, *419*, 133–141. [CrossRef]
4. Salazar, J.B.; Falcone, D.D.; Pham, H.N.; Datye, A.K.; Passos, F.B.; Davis, R.J. Selective production of 1,2-propanediol by hydrogenolysis of glycerol over bimetallic Ru–Cu nanoparticles supported on TiO_2. *Appl. Catal. A Gen.* **2014**, *482*, 137–144. [CrossRef]
5. Lopez, A.; Aragón, J.A.; Hernández-Cortez, J.G.; Mosqueira, M.L.; Martínez-Palou, R. Study of hydrotalcite-supported transition metals as catalysts for crude glycerol hydrogenolysis. *Mol. Catal.* **2019**, *468*, 9–18. [CrossRef]
6. Li, X.; Xiang, M.; Wu, D. Hydrogenolysis of glycerol over bimetallic Cu-Ni catalysts supported on hierarchically porous SAPO-11 zeolite. *Catal. Commun.* **2019**, *119*, 170–175. [CrossRef]
7. Grabysch, T.; Muhler, M.; Peng, B.X. The kinetics of glycerol hydrodeoxygenation to 1,2-propanediol over Cu/ZrO_2 in the aqueous phase. *Appl. Catal. A Gen.* **2019**, *576*, 47–53. [CrossRef]
8. Varghese, J.J.; Cao, L.; Robertson, C.; Yang, Y.; Gladden, L.F.; Lapkin, A.A.; Mushrif, S.H. Synergistic Contribution of the Acidic Metal Oxide–Metal Couple and Solvent Environment in the Selective Hydrogenolysis of Glycerol: A Combined Experimental and Computational Study Using ReO_x-Ir as the Catalyst. *ACS Catal.* **2019**, *9*, 485–503. [CrossRef]
9. Wan, X.; Zhang, Q.; Zhu, M.; Zhao, Y.; Liu, Y.; Zhou, C.; Yang, Y.; Cao, Y. Interface synergy between IrO_x and H-ZSM-5 in selective C–O hydrogenolysis of glycerol toward 1,3-propanediol. *J. Catal.* **2019**, *375*, 339–350. [CrossRef]
10. Liu, L.; Kawakami, S.; Nakagawa, Y.; Tamura, M.; Tomishige, K. Highly active iridium-rhenium catalyst condensed on silica support for hydrogenolysis of glycerol to 1,3-propanediol. *Appl. Catal. B Environ.* **2019**, *256*, 117775. [CrossRef]
11. Priya, S.S.; Kumar, V.P.; Kantam, M.L.; Bhargava, S.K.; Periasamy, S.; Chary, K.V.R. High Efficiency Conversion of Glycerol to 1,3-Propanediol Using a Novel Platinum–Tungsten Catalyst Supported on SBA-15. *Ind. Eng. Chem. Res.* **2015**, *498*, 88–98. [CrossRef]
12. Bhanuchander, P.; Priya, S.S.; Kumar, V.P.; Hussain, S.; Rajan, N.P.; Bhargava, S.K.; Chary, K.V.R. Direct Hydrogenolysis of Glycerol to Biopropanols over Metal Phosphate Supported Platinum Catalysts. *Catal. Lett.* **2017**, *147*, 845–855. [CrossRef]
13. Li, C.; He, B.; Ling, Y.; Tsang, C.-W.; Liang, C. Glycerol hydrogenolysis to *n*-propanol over Zr-Al composite oxide-supported Pt catalysts. *Chin. J. Catal.* **2018**, *39*, 1121–1128. [CrossRef]
14. Marinas, A.; Bruijnincx, P.; Ftouni, J.; Urbano, F.J.; Pinel, C. Sustainability metrics for a fossil- and renewable-based route for 1,2-propanediol production: A comparison. *Catal. Today* **2015**, *239*, 31–37. [CrossRef]
15. Zhu, S.; Zhu, Y.; Hao, S.; Zheng, H.; Mo, T.; Li, Y. One-step hydrogenolysis of glycerol to biopropanols over $Pt\text{-}H_4SiW_{12}O_{40}/ZrO_2$ catalysts. *Green Chem.* **2012**, *14*, 2607–2616. [CrossRef]
16. Dasari, M.A.; Kiatsimkul, P.-P.; Sutterlin, W.R.; Suppes, G.J. Low-pressure hydrogenolysis of glycerol to propylene glycol. *Appl. Catal. A Gen.* **2005**, *281*, 225–231. [CrossRef]
17. Miyazawa, T.; Kusunoki, Y.; Kunimori, K.; Tomishige, K. Glycerol conversion in the aqueous solution under hydrogen over Ru/C + an ion-exchange resin and its reaction mechanism. *J. Catal.* **2006**, *240*, 213–221. [CrossRef]
18. Furikado, I.; Miyazawa, T.; Koso, S.; Shimao, A.; Kunimori, K.; Tomishige, K. Catalytic performance of Rh/SiO_2 in glycerol reaction under hydrogen. *Green Chem.* **2007**, *9*, 582–588. [CrossRef]
19. Van Ryneveld, E.; Mahomed, A.S.; Van Heerden, P.S.; Friedrich, H.B. Direct Hydrogenolysis of Highly Concentrated Glycerol Solutions Over Supported Ru, Pd and Pt Catalyst Systems. *Catal. Lett.* **2011**, *141*, 958–967. [CrossRef]
20. Van Ryneveld, E.; Mahomed, A.S.; Van Heerden, P.S.; Green, M.J.; Friedrich, H.B. A catalytic route to lower alcohols from glycerol using Ni-supported catalysts. *Green Chem.* **2011**, *13*, 1819–1827. [CrossRef]

21. Mai, C.T.Q.; Ng, F.T.T. Effect of Metals on the Hydrogenolysis of Glycerol to Higher Value Sustainable and Green Chemicals Using a Supported HSiW Catalyst. *Org. Process. Res. Dev.* **2016**, *20*, 1774–1780. [CrossRef]
22. Gallegos-Suarez, E.; Pérez-Cadenas, M.; Guerrero-Ruiz, A.; Rodriguez-Ramos, I.; Arcoya, A. Effect of the functional groups of carbon on the surface and catalytic properties of Ru/C catalysts for hydrogenolysis of glycerol. *Appl. Surf. Sci.* **2013**, *287*, 108–116. [CrossRef]
23. Wang, M.; Yang, H.; Xie, Y.; Wu, X.; Chen, C.; Ma, W.; Dong, Q.; Hou, Z. Catalytic transformation of glycerol to 1-propanol by combining zirconium phosphate and supported Ru catalysts. *RSC Adv.* **2016**, *6*, 29769–29778. [CrossRef]
24. Delgado, S.N.; Yap, D.; Vivier, L.; Especel, C. Influence of the nature of the support on the catalytic properties of Pt-based catalysts for hydrogenolysis of glycerol. *J. Mol. Catal. A Chem.* **2013**, *367*, 89–98. [CrossRef]
25. Zhu, S.; Qiuc, Y.; Zhu, Y.; Hao, S.; Zheng, H.; Li, Y. Hydrogenolysis of glycerol to 1,3-propanediol over bifunctional catalysts containing Pt and heteropolyacids. *Catal. Today* **2013**, *212*, 120–126. [CrossRef]
26. Musolino, M.G.; Scarpino, L.A.; Mauriello, F.; Pietropaolo, R. Glycerol Hydrogenolysis Promoted by Supported Palladium Catalysts. *ChemSusChem* **2011**, *4*, 1143–1150. [CrossRef]
27. Li, Y.; Liu, H.; Ma, L.; He, D. Influence of Pd precursors and Cl addition on performance of Pd-Re catalysts in glycerol hydrogenolysis to propanediols. *Appl. Catal. A Gen.* **2016**, *522*, 13–20. [CrossRef]
28. Samudrala, S.P.; Bhattacharya, S. Toward the Sustainable Synthesis of Propanols from Renewable Glycerol over MoO_3-Al_2O_3 Supported Palladium Catalysts. *Catalysts* **2018**, *8*, 385. [CrossRef]
29. Shozi, M.L.; Dasireddy, V.D.B.C.; Singh, S.; Govender, A.; Mohlala, P.; Friedrich, H.B. The effect of rhenium on the conversion of glycerol to mono-alcohols over nickel catalysts under continuous flow conditions. *Sustain. Energy Fuels* **2019**, *3*, 2038–2047. [CrossRef]
30. Shozi, M.L.; Dasireddy, V.D.B.C.; Singh, S.; Mohlala, P.; Morgan, D.J.; Friedrich, H.B. Hydrogenolysis of Glycerol to Monoalcohols over Supported Mo and W Catalysts. *ACS Sustain. Chem. Eng.* **2016**, *4*, 5752–5760. [CrossRef]
31. Lin, X.; Lv, Y.; Xi, Y.; Qu, Y.; Phillips, D.L.; Liu, C. Hydrogenolysis of Glycerol by the Combined Use of Zeolite and Ni/Al_2O_3 as Catalysts: A Route for Achieving High Selectivity to 1-Propanol. *Energy Fuels* **2014**, *28*, 3345–3351. [CrossRef]
32. Balaraju, M.; Rekha, V.; Prabhavathi Devi, B.L.A.; Prasad, R.B.N.; Sai Prasad, P.S.; Lingaiah, N. Surface and structural properties of titania-supported Ru catalysts for hydrogenolysis of glycerol. *Appl. Catal. A Gen.* **2010**, *384*, 107–114. [CrossRef]
33. Rajkhowa, T.; Marin, G.B.; Thybaut, J.W. Quantifying the dominant factors in Cu catalyst deactivation during glycerol hydrogenolysis. *J. Ind. Eng. Chem.* **2017**, *54*, 270–277. [CrossRef]
34. Balaraju, M.; Jagadeeswaraiah, K.; Sai Prasad, P.S.; Lingaiah, N. Catalytic hydrogenolysis of biodiesel derived glycerol to 1,2-propanediol over Cu-MgO catalysts. *Catal. Sci. Technol.* **2012**, *2*, 1967–1976. [CrossRef]
35. Dam, J.T.; Kapteijn, F.; Djanashvili, K.; Hanefeld, U. Tuning selectivity of Pt/$CaCO_3$ in glycerol hydrogenolysis-A Design of Experiments approach. *Catal. Commun.* **2011**, *13*, 1–5. [CrossRef]
36. Gatti, M.N.; Mizrahi, M.D.; Ramallo-Lopez, J.M.; Pompeo, F.; Santori, G.F.; Nichio, N.N. Improvement of the catalytic activity of Ni/SiO_2-C by the modification of the support and Zn addition: Bio-propylene glycol from glycerol. *Appl. Catal. A Gen.* **2017**, *548*, 24–32. [CrossRef]
37. Gatti, M.N.; Pompeo, F.; Santori, G.F.; Nichio, N.N. Bio-propylene glycol by liquid phase hydrogenolysis of glycerol with Ni/SiO_2-C catalysts. *Catal. Today* **2017**, *296*, 26–34. [CrossRef]
38. Snaz, J.; Campelo, J.M.; Marinas, J.M. NMR characterization of synthetic and modified aluminum orthophosphates. *J. Catal.* **1991**, *130*, 642–652. [CrossRef]
39. Campelo, J.M.; Jaraba, M.; Luna, D.; Luque, R.; Marinas, J.M.; Romero, A.A. Effect of Phosphate Precursor and Organic Additives on the Structural and Catalytic Properties of Amorphous Mesoporous $AlPO_4$ Materials. *Chem. Mater.* **2003**, *15*, 3352–3364. [CrossRef]
40. Raddi de Araujo, L.R.; Scofield, C.F.; Pastura, N.M.R.; Gonzalez, W.A. H_3PO_4/Al_2O_3 Catalysts: Characterization and Catalytic Evaluation of Oleic Acid Conversion to Biofuels and Biolubricant. *Mater. Res.* **2006**, *9*, 181–184. [CrossRef]
41. Gervasini, A.; Fenyvesi, J.; Auroux, A. Study of the acidic character of modified metal oxide surfaces using the test of isopropanol decomposition. *Catal. Lett.* **1997**, *43*, 219–228. [CrossRef]
42. Moffat, J.B.; Vetrivel, R.; Viswanathan, B. A model cluster study of the acid-base properties of phosphate catalysts. *J. Mol. Catal.* **1985**, *30*, 171–180. [CrossRef]

43. Nahil, M.A.; Williams, P.T. Pore characteristics of activated carbons from the phosphoric acid chemical activation of cotton stalks. *Biomass Bioenergy* **2012**, *37*, 142–149. [CrossRef]
44. Yang, Y.; Ochoa-Hernández, C.; Pizarro, P.; De la Peña O'Shea, V.A.; Coronado, J.M.; Serrano, D.P. Influence of the Ni/P ratio and metal loading on the performance of Ni_xP_y/SBA-15 catalysts for the hydrodeoxygenation of methyl oleate. *Fuel* **2015**, *144*, 60–70. [CrossRef]
45. Cecilia, J.A.; Infantes-Molina, A.; Rodríguez-Castellón, E.; Jiménez-López, A. A novel method for preparing an active nickel phosphide catalyst for HDS of dibenzothiophene. *J. Catal.* **2009**, *263*, 4–15. [CrossRef]
46. Senseni, A.Z.; Meshkani, F.; Rezaei, M. Steam reforming of glycerol on mesoporous nanocrystalline Ni/Al_2O_3 catalysts for H_2 production. *Int. J. Hydrogen Energy* **2016**, *41*, 20137–20146. [CrossRef]
47. Wu, G.; Zhang, C.; Li, S.; Han, Z.; Wang, T.; Ma, X.; Gong, J. Hydrogen Production via Glycerol Steam Reforming over Ni/Al_2O_3: Influence of Nickel Precursors. *ACS Sustain. Chem. Eng.* **2013**, *1*, 1052–1062. [CrossRef]
48. Guo, J.; Lou, H.; Zhao, H.; Chai, D.; Zheng, X. Dry reforming of methane over nickel catalysts supported on magnesium aluminate spinels. *Appl. Catal. A Gen.* **2004**, *273*, 75–82. [CrossRef]
49. Marinoiu, A.; Ionita, G.; Gaspar, C.L.; Cobzaru, C.; Oprea, S. Glycerol hydrogenolysis to propylene glycol. *React. Kinet. Catal. Lett.* **2009**, *97*, 315–320. [CrossRef]
50. Menchavez, R.N.; Morra, M.J.; He, B.B. Co-Production of Ethanol and 1,2-Propanediol via Glycerol Hydrogenolysis Using Ni/Ce–Mg Catalysts: Effects of Catalyst Preparation and Reaction Conditions. *Catalysts* **2017**, *7*, 290. [CrossRef]
51. Long, W.; Hao, F.; Xiong, W.; Liu, P.; Luo, H. Modified sepiolite supported nickel and tungsten oxide catalysts for glycerol hydrogenolysis to 1,2-propanediol with high selectivity under mild conditions. *React. Kinet. Mech. Catal.* **2017**, *122*, 85–100. [CrossRef]
52. Perosa, A.; Tundo, P. Selective Hydrogenolysis of Glycerol with Raney Nickel. *Ind. Eng. Chem. Res.* **2005**, *44*, 8535–8537. [CrossRef]
53. Zhao, J.; Yu, W.; Chen, C.; Miao, H.; Ma, H.; Xu, J. Ni/NaX: A Bifunctional Efficient Catalyst for Selective Hydrogenolysis of Glycerol. *Catal. Lett.* **2010**, *134*, 184–189. [CrossRef]
54. Feng, J.; Wang, J.; Zhou, Y.; Fu, H.; Chen, H.; Li, X. Effect of Base Additives on the Selective Hydrogenolysis of Glycerol over Ru/TiO_2 Catalyst. *Chem. Lett.* **2007**, *36*, 1274–1275. [CrossRef]
55. Gandarias, I.; Arias, P.L.; Fernandez, S.G.; Requies, J.; Doukkali, M.E.; Guemez, M.B. Hydrogenolysis through catalytic transfer hydrogenation: Glycerol conversion to 1,2-propanediol. *Catal. Today* **2012**, *195*, 22–31. [CrossRef]
56. Lee, Y.-K.; Oyama, S.T. Bifunctional nature of a SiO_2-supported Ni_2P catalyst for hydrotreating: EXAFS and FTIR studies. *J. Catal.* **2006**, *239*, 376–389. [CrossRef]
57. Sawhill, S.; Layman, K.; Vanwyk, D.; Engelhard, M.; Wang, C.; Bussell, M. Thiophene hydrodesulfurization over nickel phosphide catalysts: Effect of the precursor composition and support. *J. Catal.* **2005**, *231*, 300–313. [CrossRef]
58. Chen, J.; Shi, H.; Li, L.; Li, K. Deoxygenation of methyl laurate as a model compound to hydrocarbons on transition metal phosphide catalysts. *Appl. Catal. B Environ.* **2014**, *144*, 870–884. [CrossRef]
59. Zhao, S.; Li, M.; Chu, Y.; Chen, J. Hydroconversion of Methyl Laurate as a Model Compound to Hydrocarbons on Bifunctional Ni_2P/SAPO-11: Simultaneous Comparison with the Performance of Ni/SAPO-11. *Energy Fuels* **2014**, *28*, 7122–7132. [CrossRef]
60. Scanlon, J.T.; Willis, D.E. Calculation of Flame Ionization Detector Relative Response Factors Using the Effective Carbon Number Concept. *J. Chromatogr. Sci.* **1985**, *23*, 333–340. [CrossRef]